

Radiation-enhanced diffusion of impurity atoms in silicon layers

O. I. Velichko

E-mail address (Oleg Velichko): velichkomail@gmail.com

Abstract Modeling of the phosphorus radiation-enhanced diffusion in the course of implantation of high-energy protons into an elevated-temperature silicon substrate and during its treatment in a hydrogen-containing plasma with addition of a diffusant has been carried out. It follows from the results obtained that the radiation-enhanced diffusion occurs by means of formation, migration, and dissociation of “impurity atom – silicon self-interstitial” pairs being in a local thermodynamic equilibrium with substitutionally dissolved impurity atoms and nonequilibrium point defects generated due to external irradiation.

The resulting value of the average migration length of nonequilibrium silicon self-interstitials decreases from $0.19\ \mu\text{m}$ for proton energy of 140 keV to 0.09 and $0.08\ \mu\text{m}$ for energies of 110 and 80 keV, respectively. The decrease of the average migration length with the proton energy can be due to the interaction of silicon self-interstitials with the vacancies generated at the surface or with the defects formed in the phosphorus implanted region.

Based on the pair diffusion mechanism, a theoretical investigation of the form of impurity profiles that can be created in thin silicon layers due to the radiation-enhanced diffusion was carried out. It is shown that depletion of the uniformly doped silicon layer occurs during plasma treatment except for the silicon – insulator interface where a narrow region with a high impurity concentration is formed. The results of calculations give a clear evidence in favor of further investigation of various doping processes based on the radiation-enhanced diffusion, especially the processes of plasma doping, to develop a cheap method for the formation of strictly assigned impurity distributions in the local semiconductor domains.

1 Introduction

An important trend in the present-day electronics is the diminishing of the dimensions of semiconductor devices [1]. Now, the active regions of advanced integrated microcircuits and optoelectronics devices can reach geometric dimensions of about 10 nm. Another trend is the use of diverse multilayer structures to achieve the required parameters of devices. The multilayer structures are employed in the devices based on compound semiconductors, silicon or germanium. For example, much attention has been paid recently to engineering $\text{Ge}_{1-x}\text{Si}_x$ layers [2, 3, 4, 5] and to the silicon on insulator technology (SOI) [6, 7, 8]. The implementation of these trends means that interfaces will exert a significant influence on the dopant–defect system and, consequently, on the electrophysical parameters of devices. For example, the interfaces present themselves as planar defects and can act as a source [9] or sink of point defects [10]. Thus, distributions of point defects can be nonuniform in the vicinity of the interface. Nonuniform distributions of nonequilibrium point defects can also be formed due to ion implantation that is widely used for the

production of modern microcircuits and other electronic devices [11]. If the concentration of point defects generated due to ion implantation or ion bombardment exceeds the thermally equilibrium concentration, the radiation-enhanced diffusion (RED) occurs.

The present analysis of the up-to-date trends in the modern technology of electronic devices allows the formulation of the main idea of the proposed theoretical investigation. The goal of this work is to describe the main features of a coupled evolution of dopant–defect system in thin silicon layers resulting from the nonuniformity of point defect distributions formed due to the surface influence or due to ion implantation (bombardment). The expected results will be important for the design of devices as well as for the semiconductor physics and technology.

2 Models of the radiation-enhanced diffusion

The equation describing the impurity diffusion due to the formation, migration, and dissociation of the “impurity atom – vacancy” and “impurity atom – silicon self-interstitial” pairs has been obtained earlier in [12]. It was supposed that nonuniform distributions of point defects, including defects in the neutral charge state, can be formed and that the mass action law is valid for the substitutionally dissolved impurity atoms, nonequilibrium self-interstitials or vacancies, and the pairs. The equation takes account of different charge states of all mobile and immobile species and the drift of the pairs and point defects in a built-in electric field, although only the concentrations of neutral point defects are involved in an explicit form. In the case of low impurity concentration $C \leq n_i$, the equation obtained can be presented in the form

$$\frac{\partial C}{\partial t} = D_i^E \Delta \left(\tilde{C}^{V\times} C \right) + D_i^F \Delta \left(\tilde{C}^{I\times} C \right). \quad (1)$$

Here C is the concentration of substitutionally dissolved impurity atoms, n_i is the intrinsic carrier concentration, D_i^E and D_i^F are the diffusivities of impurity atoms in intrinsic silicon due to the “impurity atom – vacancy” and “impurity atom – silicon self-interstitial” pairs, respectively, $\tilde{C}^{V\times}$ and $\tilde{C}^{I\times}$ are the concentrations of vacancies and silicon interstitial atoms in the neutral charge state normalized to the thermally equilibrium concentrations of these species, $C_{eq}^{V\times}$ and $C_{eq}^{I\times}$, respectively. It is worth noting that $\tilde{C}^{V\times} = \tilde{C}^V$ and $\tilde{C}^{I\times} = \tilde{C}^I$ for the low impurity concentration $C \leq n_i$. Here \tilde{C}^V and \tilde{C}^I are respectively the total concentrations of vacancies and silicon interstitial atoms normalized to the thermally equilibrium concentrations of these species, C_{eq}^V and C_{eq}^I .

For a number of doping processes only one kind of defect is involved in diffusion of the main fraction of impurity atoms [9]. Then, Eq. (1) can be presented in a simplified form:

$$\frac{\partial C}{\partial t} = D_i \Delta \left(\tilde{C}^\times C \right), \quad (2)$$

where \tilde{C}^\times is the concentration of the neutral defects responsible for impurity diffusion normalized to the thermally equilibrium concentration of this species, .

The equation obtained retains the basic character of the original equations presented in [12], namely, the ability to describe segregation of impurity atoms, including “uphill” impurity diffusion. Indeed, we shall present Eq. (2) in the following form:

$$\frac{\partial C}{\partial t} = D_i \nabla \left(\tilde{C}^\times \nabla C \right) + D_i \nabla \left[\left(\nabla \tilde{C}^\times \right) C \right]. \quad (3)$$

It is clearly seen from Eq. (3) that, depending on the gradient of the concentration of neutral point defects, the drift term is added to the right hand side of the equation, which has the type of the Fick second law. It means that an additional drift flux of impurity atoms proportional to the gradient of concentration of point defects in a neutral charge state is added to the flux caused by a gradient of the impurity concentration. If these fluxes are opposite-directed, a component of “uphill” diffusion is included to the general impurity flux. It means that segregation of impurity atoms can be observed at great values of the gradient of point defects in a neutral charge state instead of the leveling effect for nonuniform impurity distribution. If the “uphill” diffusion component exceeds the usual diffusion flux, described by the Fick first law, an unusual form of impurity profile is observed. Therefore, by modeling the impurity diffusion under conditions of nonuniform distribution of point defects one can obtain very useful information on the microscopic mechanisms underlying the impurity atoms and point defects migration.

In one dimension, Eqs. (2) and (3) have the following form:

$$\frac{\partial C}{\partial t} = D_i \frac{\partial^2 \left(\tilde{C}^\times C \right)}{\partial x^2} \quad (4)$$

$$\frac{\partial C}{\partial t} = D_i \frac{\partial}{\partial x} \left(\tilde{C}^\times \frac{\partial C}{\partial x} \right) + D_i \frac{\partial}{\partial x} \left(\frac{\partial \tilde{C}^\times}{\partial x} C \right). \quad (5)$$

It is worth noting that there is no difference in the mathematical description of impurity transport processes occurring due to equilibrium “impurity atom – silicon self-interstitial” pairs and due to the kick-out mechanism if the impurity interstitials are in local thermodynamic equilibrium with the substitutional impurity atoms and nonequilibrium silicon self-interstitials [13, 14]. At the same time, there is an essential difference between the mathematical descriptions of impurity transport caused by the equilibrium impurity-vacancy pairs and by the simple vacancy mechanism of diffusion when the impurity atom and neighboring vacancy exchange places. Indeed, the equation of impurity diffusion due to such a simple vacancy mechanism has been derived in [15, 16]:

$$\frac{\partial C}{\partial t} = D_i \frac{\partial}{\partial x} \left(\tilde{C}^v \frac{\partial C}{\partial x} \right) - D_i \frac{\partial}{\partial x} \left(\frac{\partial \tilde{C}^v}{\partial x} C \right). \quad (6)$$

It can be seen from this equation that the second term in the right-hand side of it has the “minus” sign, whereas the second term in the right-hand side of Eq. (5) has the “plus” sign. It means that the flux caused by the vacancy gradient in the simple vacancy mechanism has an opposite direction in comparison with the similar flux for the case of impurity diffusion due to impurity-vacancy pairs.

3 Preliminary studies of the radiation-enhanced diffusion

It follows from the analysis of Eqs. (5) and (6) that investigation of impurity redistribution under conditions of nonuniform distribution of the point defects responsible for the impurity diffusion allows one to draw a conclusion regarding the character of the diffusion mechanism. For example, by simulating the impurity redistribution investigated in [17], it was shown in [18] that the radiation-enhanced diffusion of boron during proton bombardment of a silicon substrate having an elevated temperature occurs due to the equilibrium “impurity atom – intrinsic point defect” pairs. It follows from [19, 20] that the vacancy-type defects are formed in the region between the surface and the average projective range of implanted ions R_p (more exactly, in the vicinity of $R_p/2$), whereas the interstitial stacking faults are formed near R_p and deeper inside. For a proton energy of 140 keV used for boron redistribution in [17], $R_p = 1.235 \mu\text{m}$ and $R_m = 1.27 \mu\text{m}$ [21]. Here R_p is the average projective range of implanted ions and R_m is the position of the maximum for concentration profile of implanted protons described by the type IV Pearson distribution [21]. Taking into account the experimental results of [19, 20], one can conclude that silicon self-interstitials are the point defects responsible for the RED of boron atoms, because the local minimum of impurity concentration profile (both experimental and theoretical) lies near R_m .

We have a more complicated situation for the radiation-enhanced diffusion of phosphorus atoms. Indeed, in [22, 23] simulation of phosphorus redistribution during proton bombardment of doped silicon substrates was carried out. The experimental data of [17] were used for comparison. In the experiments of Akutagawa et al. [17] the initial phosphorus profile in the (111) oriented silicon substrates was formed due to ion implantation with an energy of 140 keV and a dose of 1.5×10^{12} ions/cm². The choice of a very low dose was necessary for phosphorus profiling by the differential C-V technique to avoid the effects caused by avalanche breakdown. Simultaneously, the effects caused by the concentration-dependent diffusion were avoided. After the implantation and before the proton-enhanced diffusion, the wafers were annealed at a temperature of 750 °C for 30 min in a purified argon ambient for electrical activation of the implanted impurity. After the enhanced diffusion, the samples were left in the target chamber at 700 °C for times longer than about 30 min for postannealing treatment, which is expected to produce full electrical activity of the impurity and remove the residual radiation damage. To provide the radiation-enhanced diffusion, the silicon substrates were implanted with 80-keV protons at a beam density of $1.0 \mu\text{A}/\text{cm}^2$. Proton bombardment was carried out at a temperature of 700 °C for 3, 10, 30, and 120 minutes. It was concluded from the simulation results that the RED of phosphorus atoms is governed by the “impurity atom – intrinsic point defect” pairs that are in local equilibrium with the substitutionally dissolved phosphorus and generated point defects. In contrast to the boron enhanced diffusion, it was found that the maximum of point defect generation rate as well as the local minimum of the impurity concentration profile are located near R_{mD} , where R_{mD} is the position of the maximum of the energy deposited in atomic collisions in silicon under proton bombardment [24]. As follows from [24], the value of $R_{mD} = 0.6782 \mu\text{m}$ is less than the value of $R_m = 0.7922 \mu\text{m}$. Taking into account [19, 20], one can conclude that the vacancies are rather the point defects responsible for the RED of phosphorus, whereas nonequilibrium

silicon self-interstitials provide boron diffusion. Unfortunately, in [22, 23] an approximate analytical solution was used to calculate the point defect distribution. Therefore, it is reasonable to investigate the radiation-enhanced diffusion of phosphorus atoms more thoroughly.

4 Simulation of phosphorus radiation-enhanced diffusion

4.1 Diffusion due to the exchange of places between an impurity atom and a neighboring vacancy

Let us first exclude the simple vacancy mechanism of diffusion when the exchange of places between an impurity atom and a neighboring vacancy occurs. For this purpose we can use the experimental data of Strack [25] that were obtained for the case of a long-term treatment when the sputtering of the surface of a semiconductor plays a significant role and, therefore, the distribution of impurity atoms becomes stationary. In the experiments of [25] the *p*-type silicon with a conductivity of 200 Ω cm was used. The treatment temperature was equal to 820 °C and the rate of surface sputtering was equal approximately to 5.28×10^{-4} μ m/s. The impurity distribution profile was found by removing thin layers from the surface of a sample and measuring their sheet resistance. The thermal diffusivity of phosphorus at the above-mentioned temperature is equal to 1.919×10^{-8} μ m²/s [28], the intrinsic carrier concentration, to $n_i = 2.76 \times 10^6$ μ m⁻³.

In order to calculate the impurity distribution measured in [25], it is reasonable to introduce a new coordinate system, $x = x^* - v_s t$, bound to the moving surface of the semiconductor and solve the diffusion equation in this mobile coordinate system. Here x^* is the coordinate measured from the initial position of the semiconductor surface, v_s is the projection of the surface velocity on the immobile axis x^* ($v_s > 0$ in the case of sputtering of the surface).

Then, the equation of impurity diffusion (6) in the moving coordinate system takes the following form:

$$\frac{\partial C}{\partial t} = D_i \frac{\partial}{\partial x} \left(\tilde{C}^V \frac{\partial C}{\partial x} \right) - D_i \frac{\partial}{\partial x} \left(\frac{\partial \tilde{C}^V}{\partial x} C \right) + v_s \frac{\partial C}{\partial x}. \quad (7)$$

When the impurity atoms entering from the plasma are compensated by those removed from the semiconductor surface due to sputtering, the distributions of the impurity atoms and vacancies become stationary in the moving system of coordinates. Then, Eq. (7) will be transformed into a stationary diffusion equation:

$$D_i \frac{d}{dx} \left(\tilde{C}^V \frac{dC}{dx} \right) - D_i \frac{d}{dx} \left(\frac{d\tilde{C}^V}{dx} C \right) + v_s \frac{dC}{dx} = 0. \quad (8)$$

The ordinary differential equation (8) can be solved analytically. Let us obtain such an analytical solution for the following Dirichlet boundary conditions:

$$C(0) = C_s, \quad C(+\infty) = 0, \quad (9)$$

where C_S is the impurity concentration on the semiconductor surface.

To obtain an analytical solution of the boundary-value problem formulated, let us present Eq. (8) in the following form:

$$\frac{d}{dx} \left[D_i \tilde{C}^V \frac{dC}{dx} - D_i \left(\frac{d\tilde{C}^V}{dx} \right) C + v_S C \right] = 0 \quad (10)$$

and integrate (10) from x to $+\infty$ to obtain

$$D_i \tilde{C}^V \frac{dC}{dx} \Big|_x^{+\infty} - D_i \left(\frac{d\tilde{C}^V}{dx} \right) C \Big|_x^{+\infty} + v_S C \Big|_x^{+\infty} = 0. \quad (11)$$

As soon as both the impurity and vacancies concentrations as well as their fluxes are equal to zero on the right boundary $x = +\infty$, the ordinary differential equation can be obtained from Eq. (11):

$$D_i \tilde{C}^V \frac{dC}{dx} - D_i \left(\frac{d\tilde{C}^V}{dx} \right) C + v_S C = 0. \quad (12)$$

This equation can be solved using the separation of variables:

$$\frac{dC(x)}{C(x)} = \frac{\frac{d\tilde{C}^V(x)}{dx} - \frac{v_S}{D_i}}{\tilde{C}^V(x)} dx. \quad (13)$$

Let us integrate Eq. (13) from 0 to x :

$$\ln [C(x)] \Big|_0^x = \ln [\tilde{C}^V(x)] \Big|_0^x - \frac{v_S}{D_i} \int_0^x \frac{1}{\tilde{C}^V(x)} dx, \quad (14)$$

or

$$\ln \left[\frac{C(x)}{C_S} \right] = \ln \left[\frac{\tilde{C}^V(x)}{\tilde{C}_S^V} \right] - \frac{v_S}{D_i} \int_0^x \frac{1}{\tilde{C}^V(x)} dx, \quad (15)$$

where \tilde{C}_S^V is the normalized concentration of vacancies on the semiconductor surface.

Using exponentiation of Eq. (15), we obtain the expression for the distribution of impurity concentration in the form

$$C(x) = C_S \frac{\tilde{C}^V(x)}{\tilde{C}_S^V} \exp \left[-\frac{v_S}{D_i} \int_0^x \frac{1}{\tilde{C}^V(x)} dx \right]. \quad (16)$$

It follows from expression (16) that for $v_S \geq 0$ the concentration of impurity atoms $C(x) \rightarrow 0$ at $\tilde{C}^V(x) \rightarrow 0$. Let us consider the widespread case of defect generation on the semiconductor surface. Then, the spatial distribution of vacancies can be described by the expression

$$\tilde{C}^V(x) = \tilde{C}_S^V \exp \left[-\frac{x}{l_i^V} \right], \quad (17)$$

where $l_i^V = \sqrt{d_i^V \tau_i^V}$ is the average migration length of nonequilibrium point defects. Here d_i^V and τ_i^V are the diffusivity and average lifetime of vacancies in intrinsic silicon, respectively.

Substituting (17) into (16) and calculating the integral obtained, we find that the impurity distribution is determined by the expression

$$C(x) = C_S \frac{\tilde{C}^V(x)}{\tilde{C}_S^V} \exp \left\{ -\frac{v_S l_i^V}{D_i \tilde{C}_S^V} \left[\exp \left(\frac{x}{l_i^V} \right) - 1 \right] \right\}. \quad (18)$$

The phosphorus concentration profile calculated by means of expression (18) for silicon doping from the gas discharge plasma is presented in Fig. 1. The average migration length of point defects l_i^V was chosen to be equal to $0.34 \mu\text{m}$.

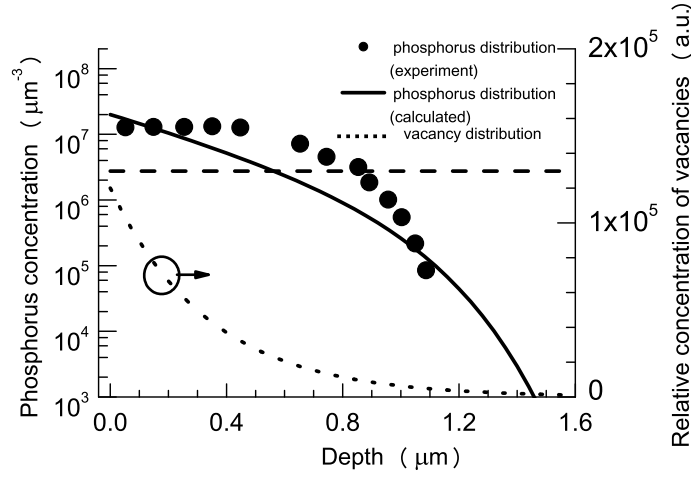


Figure 1: Calculated phosphorus profile for radiation-enhanced diffusion due to plasma treatment at a temperature of 820°C . The dotted curve is the concentration of nonequilibrium point defects normalized to the thermally equilibrium one. The filled circles represent the experimental phosphorus profile from [25]. The dashed curve is the concentration of intrinsic carriers. It is supposed that the diffusion of phosphorus occurs due to the simple vacancy mechanism

As can be seen from Fig. 1, the impurity concentration profile calculated from expression (18) disagrees qualitatively with the experimental data describing the phosphorus radiation-enhanced diffusion. Therefore, one can conclude that the simple vacancy mechanism does not play an important role in the phosphorus diffusion. On the other hand, the assumption that the phosphorus diffusion occurs due to the “impurity atom – intrinsic point defect” pairs provides an excellent agreement between the calculated and experimental concentration profiles for the phosphorus radiation-enhanced diffusion [26]. The agreement is observed in the entire diffusion zone including the region near the semiconductor surface.

4.2 Diffusion due to the formation, migration, and dissociation of “impurity atom – intrinsic point defect” pairs

For simulation of the RED of phosphorus atoms within the framework of the pair diffusion mechanism we use the experimental data of [17] similar to investigations of [22, 23]. However, in contrast to [22] another set of the data was chosen, namely, the phosphorus concentration profiles obtained for different values of proton bombardment energy. To improve the fitting to the experimental impurity profiles before and after the radiation-enhanced diffusion, it was supposed that, due to the impurity implantation and also to the proton bombardment, relatively small amounts of phosphorus atoms occupy an interstitial position and participate in the long-range interstitial diffusion [27]. It is worth noting that preliminary simulation shows that the average migration length of point defects decreases with the proton energy. This phenomenon can be explained if we suppose that the point defects responsible for the RED interact with sinks located in the phosphorus-implanted layer or annihilate with the nonequilibrium point defects generated at the surface or in the layer damaged by phosphorus implantation. We suppose that additional point defects are generated because simulation shows that there is an additional redistribution of implanted impurity directed to the region of implanted protons. For example, if the radiation-enhanced diffusion is governed by silicon self-interstitials, vacancies can be these additional point defects according to the investigations of [19, 20]. We propose, for simplicity, that these defect are generated on the surface, but this problem requires a further investigation. With the assumptions made above, the total flux of phosphorus is the sum of the E-center flux and of the “phosphorus atom – silicon self-interstitial” pairs flux. To simulate this process, the diffusion equation obtained in [12] can be used. In one dimension, Eq. (1) has the following form:

$$\frac{\partial C}{\partial t} = D_i^E \frac{\partial^2 (\tilde{C}^{V \times C})}{\partial x^2} + D_i^F \frac{\partial^2 (\tilde{C}^{I \times C})}{\partial x^2}. \quad (19)$$

The phosphorus concentration profiles calculated for the radiation-enhanced diffusion owing its origin to the pair diffusion mechanism described by Eq. (19) are presented in Figs. 2, 3, and 4. The energy of proton bombardment is equal to 140, 110, and 80 keV, respectively. Proton bombardment was carried out at a temperature of 700 °C for 2 hours at a beam density of 1.0 $\mu\text{A}/\text{cm}^2$.

To approximate the initial phosphorus concentration profile, we used the value of the dose equal to 1.7×10^{12} ions/ cm^2 that is 13.3 % larger than the dose reported in [17]. In addition, it is supposed that a small fraction of implanted impurity (5.2×10^2 ions/ cm^2) occupied an interstitial position and participated in the interstitial migration with an average migration length of 0.42 μm . Due to the long-range interstitial migration during implantation and subsequent annealing, a “tail” region of the initial phosphorus profile is formed. The interstitial phosphorus atoms also form a “tail” region of the final impurity profile. The dose of phosphorus interstitials generated during proton bombardment is equal to 7.4×10^2 ions/ cm^2 .

The following values of parameters that describe the implantation of 140 keV hydrogen ions have been used for calculating the phosphorus concentration profile presented in Fig. 2: $R_p = 1.24 \mu\text{m}$, $\Delta R_p = 0.131 \mu\text{m}$, $Sk = -5.44$, $R_m = 1.31 \mu\text{m}$ [21]. Here R_p and ΔR_p are the average projective range of implanted ions and straggling of the projective

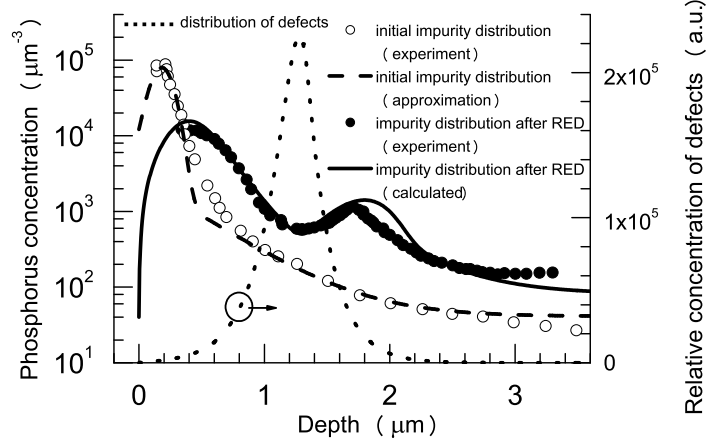


Figure 2: Calculated phosphorus concentration profile for the radiation-enhanced diffusion under conditions of proton implantation with an energy of 140 keV at a temperature of 700 °C for 2 hours. The dashed and solid curves are respectively the calculated distributions of phosphorus atoms before and after diffusion, the open and filled circles are the experimental phosphorus concentration profiles according to [17], the dotted curve represents the concentration of nonequilibrium silicon self-interstitials normalized to the thermally equilibrium one

range, respectively, Sk and R_m are the skewness and the position of the maximal value of the implanted ion profile, respectively. It was supposed that the generation rate of the nonequilibrium point defects responsible for the diffusion of impurity atoms is proportional to the distribution of implanted protons. The value of the intrinsic phosphorus diffusivity $= 4.849 \times 10^{-10} \mu\text{m}^2/\text{s}$ has been calculated from the temperature dependence presented in [28]. It is supposed that a fraction of intrinsic diffusivity referred to as the diffusion due to the “impurity atom – silicon self-interstitial” pairs is equal to $4.0 \times 10^{-10} \mu\text{m}^2/\text{s}$, whereas a fraction related to the “impurity atom – vacancy” pairs (E-centers) is much smaller ($0.849 \times 10^{-10} \mu\text{m}^2/\text{s}$). The Robin-type boundary condition providing the removal of a part of phosphorus atoms was imposed on the semiconductor surface.

The stationary distribution of nonequilibrium defects was obtained from the numerical solution of the diffusion equation for point defects and is presented in Fig. 2 by a dotted curve (silicon self-interstitials). The average migration length of silicon self-interstitials in intrinsic silicon $l_i^I = \sqrt{d_i^I \tau_i^I}$, derived from the fitting of the calculated phosphorus concentration profile after diffusion to the experimental one, is equal to $0.19 \mu\text{m}$. Here d_i^I and τ_i^I are the diffusivity and average lifetime of silicon self-interstitials in intrinsic silicon, respectively. It follows from this fitting that the average migration length of vacancies is equal to $0.3 \mu\text{m}$ if they are generated on the semiconductor surface with a normalized surface concentration equal to $1.7 \times 10^5 \text{ a.u.}$

It can be seen from Fig. 2 that there is a good agreement between the calculated and experimental phosphorus concentration profiles including the position of the local minimum of impurity concentration and the form of “uphill” diffusion region. Similar calculations for a proton energy of 110 keV are presented in Fig. 3.

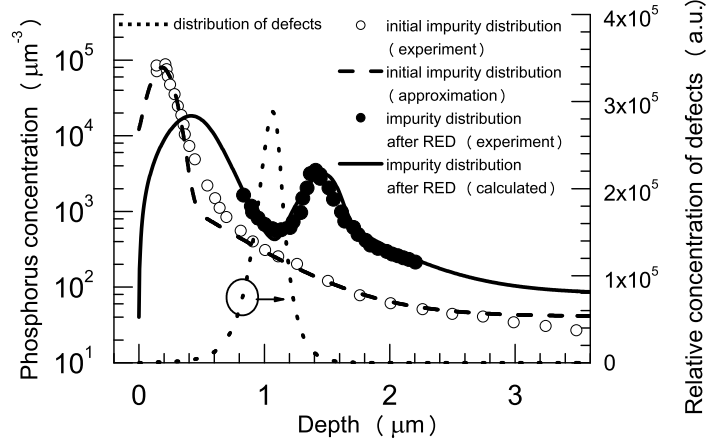


Figure 3: Calculated phosphorus concentration profile for the radiation-enhanced diffusion under conditions of proton implantation with an energy of 110 keV at a temperature of 700 °C for 2 hours. The dashed and solid curves are the calculated distributions of phosphorus atoms respectively before and after diffusion, the open and filled circles are the experimental phosphorus concentration profiles according to [17], the dotted curve represents the concentration of nonequilibrium silicon self-interstitials normalized to the thermally equilibrium one

The following values of parameters that describe the implantation of 110 keV hydrogen ions have been used for calculating the phosphorus concentration profile presented in Fig. 3: $R_p = 1.02 \mu\text{m}$, $\Delta R_p = 0.12 \mu\text{m}$, $Sk = -4.73$, and $R_m = 1.087 \mu\text{m}$. It is worth noting that the values of ΔR_p and Sk are taken from [21]. On the other hand, the value $R_p = 1.02 \mu\text{m}$ is greater than $R_p = 0.982 \mu\text{m}$ from [21]. Using the value $R_p = 0.982 \mu\text{m}$ results in a more poor agreement with experimental data, especially for the position of the local minimum on the phosphorus concentration profile. The average migration length of silicon self-interstitials l_i^I , derived from the fitting to experimental data, is equal to $0.09 \mu\text{m}$, i. e., less than the average migration length for bombardment with a proton energy of 140 keV. The dose of phosphorus interstitials generated during proton bombardment and participated in the long-range migration is equal to $9.2 \times 10^2 \text{ ions/cm}^2$. The other modeling parameters are the same as in the previous case of 140 keV proton bombardment.

Finally, the results of modeling of the radiation-enhanced diffusion for a proton energy of 80 keV are presented in Fig. 4.

The following values of parameters that describe the implantation of 80 keV hydrogen ions have been used for calculating the phosphorus concentration profile presented in Fig. 4: $R_p = 0.572 \mu\text{m}$, $\Delta R_p = 0.1092 \mu\text{m}$, $Sk = -3.96$, and $R_m = 0.6304 \mu\text{m}$. The average migration length of silicon self-interstitials l_i^I , derived from the fitting to experimental data, is equal to $0.08 \mu\text{m}$, i. e., practically it equals the average migration length for the case of bombardment with a proton energy of 110 keV. The dose of phosphorus interstitials generated during proton bombardment and participated in the long-range migration is equal to $7.4 \times 10^2 \text{ ions/cm}^2$. The vacancies are generated at the semiconductor surface with a normalized surface concentration equal to $5.0 \times 10^4 \text{ a.u.}$ The other modeling parameters

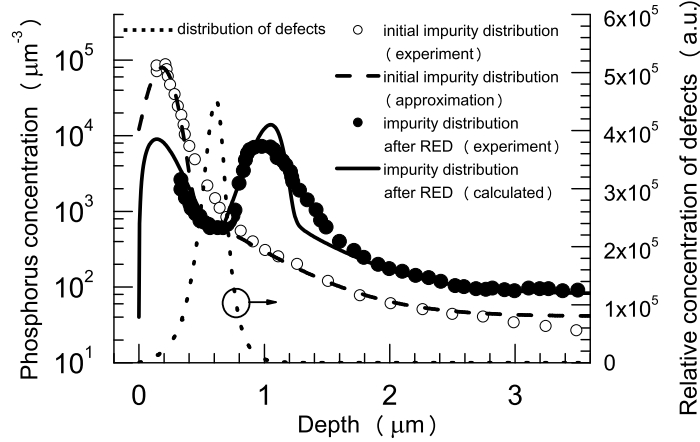


Figure 4: Calculated phosphorus concentration profile for the radiation-enhanced diffusion under conditions of proton implantation with an energy of 80 keV at a temperature of 700 °C for 2 hours. The dashed and solid curves are the calculated distributions of phosphorus atoms respectively before and after diffusion, the open and filled circles are the experimental phosphorus concentration profiles according to [17], the dotted curve represents the concentration of nonequilibrium silicon self-interstitials normalized to the thermally equilibrium one

are the same as in the previous cases of proton bombardment with energies of 140 and 110 keV.

It is worth noting that $\Delta R_p = 0.1092 \mu\text{m}$ and $Sk = -3.96$ are taken from [21]. On the other hand, the used value $R_p = 0.572 \mu\text{m}$ is less than $R_p = 0.742 \mu\text{m}$ from [21] or $R_p = 0.7499 \mu\text{m}$ from [24]. It is interesting to note that $R_p = 0.572 \mu\text{m}$, derived from the fitting procedure, is approximately equal to $R_{pD} = 0.611 \mu\text{m}$ [24], where R_{pD} is the position of the maximum for distribution of the energy deposited in atomic collisions in silicon. However, taking into account the different sign of deviation between adjustable and tabulated values of R_p for proton energies of 80 and 110 keV, we suppose that, perhaps, the reason was the inaccuracy of the measurements of the phosphorus concentration profiles in [17]. The deviation of derived and tabulated R_p also can occur due to the more complicated interaction between generated defects and previously formed defects or phosphorus atoms in the implanted layer. Further investigations of the RED on the basis of precise SIMS measurements are required to solve this interesting problem. In any case, the good agreement between the calculated and experimental phosphorus concentration profiles for different energies of proton bombardment confirms the conclusion of [22] that the low-temperature radiation-enhanced diffusion of phosphorus atoms occurs due to the formation, migration, and dissociation of “impurity atom – point defect” pairs. Relying on this knowledge, we can investigate the character form of impurity concentration profiles that can be formed due to the radiation-enhanced diffusion in the layered semiconductor structures.

5 Simulation of the radiation-enhanced diffusion in thin layers

Let us consider a 0.2- μm thick uniformly doped silicon layer formed by silicon on insulator technology. Due to the small thickness of the layer, 1 keV proton implantation from the remote hydrogen containing plasma can be used to provide radiation-enhanced diffusion. If the silicon substrate temperature is equal to 700 $^{\circ}\text{C}$, there is no passivation of impurity by hydrogen atoms [29]. The results of modeling of the radiation-enhanced diffusion phosphorus atoms for 0.5, 2, and 60 minutes are presented in Fig. 5.

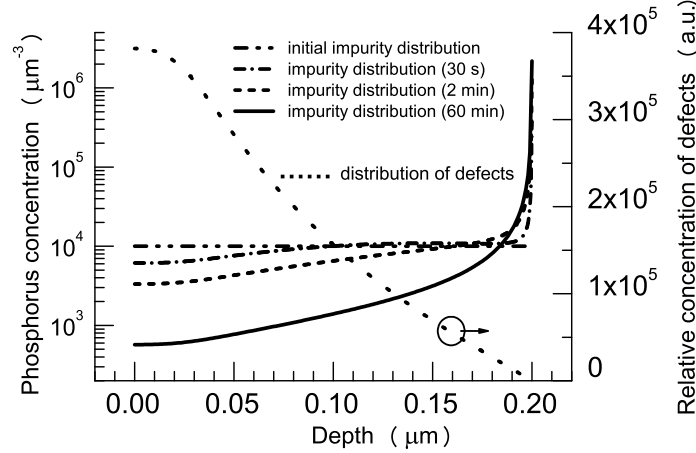


Figure 5: Calculated phosphorus concentration profiles for the radiation-enhanced diffusion under conditions of proton bombardment with an energy of 1 keV at a temperature of 700 $^{\circ}\text{C}$ for 0.5, 2, and 60 minutes. The dash-double-dotted curve represents the initial impurity distribution, the dash-dotted, dashed, and solid curves are the calculated distributions of phosphorus atoms after the radiation-enhanced diffusion for 0.5, 2, and 60 minutes, respectively, the dotted curve represents the concentration of nonequilibrium silicon self-interstitials normalized to the thermally equilibrium one

The following values of parameters that describe the implantation of 1 keV hydrogen ions have been used for calculating the phosphorus concentration profiles after the RED presented in Fig. 5: $R_p = 0.01631 \mu\text{m}$, $\Delta R_p = 0.015 \mu\text{m}$, $Sk = -0.3$, and $R_m = 0.0184 \mu\text{m}$ [24]. The average migration length of silicon self-interstitials l_i^I has been chosen to be equal to 0.09 μm . The conditions for the generation of silicon self-interstitials are similar to the previously investigated cases of phosphorus radiation-enhanced diffusion. For simplicity, reflecting boundary conditions have been chosen for impurity atoms on the interface between the silicon layer and insulator and on the semiconductor surface. It is supposed that the reflecting boundary condition is also valid for the defect diffusion near the semiconductor surface whereas the boundary condition describing the absorption of silicon self-interstitials is used at the interface between the silicon layer and insulator.

As can be seen from Fig. 5, depletion in impurity concentration occurs practically within the whole layer due to the RED. Simultaneously, a narrow region with a high

impurity concentration is formed in the vicinity of the interface between the silicon layer and insulator. In Fig. 6 a similar calculation for the Robin-type boundary condition imposed on the semiconductor surface is presented. It is supposed that the duration of the RED is equal to 10 minutes and impurity atoms can evaporate from the surface. It can be seen from Fig. 6 that for this case of the radiation-enhanced diffusion an additional decrease in the impurity concentration occurs in the near surface region due to evaporation of impurity atoms.

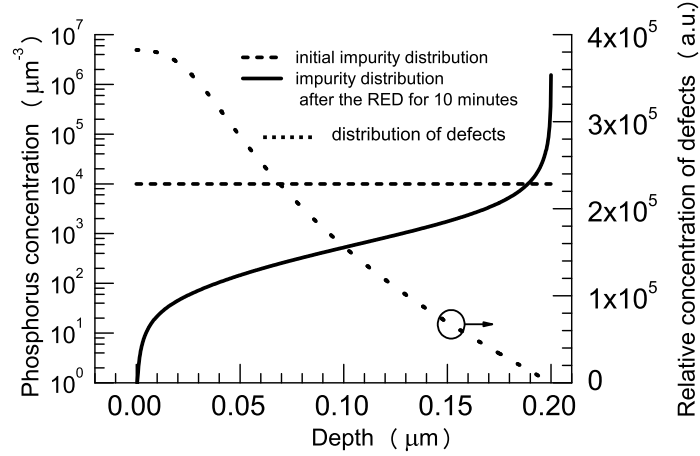


Figure 6: Calculated phosphorus concentration profiles for the radiation-enhanced diffusion under conditions of proton bombardment with an energy of 1 keV at a temperature of 700 °C for 10 minutes. The dashed and solid curves represent the initial impurity distribution and the calculated distribution of phosphorus atoms after the radiation-enhanced diffusion, respectively, the dotted curve represents the concentration of nonequilibrium silicon self-interstitials normalized to the thermally equilibrium one. It is supposed that evaporation of phosphorus atoms from the surface occurs during plasma treatment

Taking into account that strictly assigned local areas of the surface can be exposed to ion bombardment, we can form the local domains with depleted impurity concentration in the bulk and with a high concentration of impurity atoms on the boundary of these selected domains. Due to the low temperature of the radiation-enhanced diffusion, the redistribution of impurity atoms in other regions of a semiconductor will be negligible. This phenomenon can be useful for the technology of semiconductor devices and integrated microcircuits.

6 Conclusions

To investigate the microscopic mechanisms of impurity transport in semiconductors, modeling of phosphorus radiation-enhanced diffusion during implantation of high-energy protons to a silicon substrate being at an elevated temperature and during the treatment of a silicon substrate in the hydrogen-containing plasma with addition of a diffusant has been

made. It follows from the comparison of the calculated impurity profiles with experimental ones that the radiation-enhanced diffusion occurs due to the formation, migration, and dissociation of the “impurity atom – intrinsic point defect” pairs which are in a local thermodynamic equilibrium with the substitutionally dissolved impurity atoms and nonequilibrium point defects generated as a result of external irradiation. For a proton energy of 140 keV the position of the maximum of defect generation rate is equal to the maximum concentration of implanted hydrogen. This is the evidence in favor of the statement that silicon self-interstitials are the defects responsible for the phosphorus radiation-enhanced diffusion. If the proton energy decreases, the derived value of the average migration length of nonequilibrium silicon self-interstitials also decreases from 0.19 μm for an energy of 140 keV to 0.09 and 0.08 μm for energies of 110 and 80 keV, respectively. The decrease of the average migration length can occur due to the interaction of silicon self-interstitials with the vacancies generated at the surface or with the defects formed in the phosphorus implanted region. Indeed, as follows from the experimental data [17], the position of the local minimum of phosphorus concentration is shifted to the surface with proton energy decrease. This shift is a natural consequence of the decrease in the distance between the surface and position of maximum of defect generation. On the other hand, the position of the maximum of defect generation and simultaneously the maximum of the implanted hydrogen concentration $R_m = 0.6304 \mu\text{m}$ obtained by fitting the experimental phosphorus profile for a proton implantation energy of 80 keV are less than $R_m = 0.8 \mu\text{m}$ calculated from the tables in [21]. We suppose that, perhaps, there was the inaccuracy of measurements of phosphorus concentration profiles in [17]. The deviation of the derived and tabulated R_m can also occur due to the more complicated interaction between the generated defects and previously formed defects or phosphorus atoms in the implanted layer. Further investigations of the RED on the basis of precise SIMS measurements are required to solve this interesting problem.

It is worth noting that calculation for the case of simple vacancy mechanism of diffusion due to the exchange of places between the impurity atom and neighboring vacancy disagrees qualitatively with the experimental data of [25] for the phosphorus radiation-enhanced diffusion occurring during plasma treatment. To provide the latter calculation, an analytical solution of the diffusion equation that describes the quasistationary diffusion of impurity atoms under condition of the sputtering of a surface was obtained.

On the basis of the pair diffusion mechanism, a theoretical investigation was carried out for the form of impurity profiles that can be created in thin silicon layers due to the radiation-enhanced diffusion. It was shown that depletion of the uniformly doped silicon layer occurs during plasma treatment except for the vicinity of the interface between the silicon and insulator where a narrow region with a high impurity concentration is formed. These characteristic features of the dopant profile are due to the nonuniform distribution of point defects responsible for the impurity diffusion.

The results of the calculations performed give a clear evidence in favor of conducting further investigation of various doping processes based on the radiation-enhanced diffusion, especially the processes of plasma doping, to develop a cheap method for the formation of special impurity distributions in the local semiconductor domain.

References

- [1] P. A. Packan, Scaling transistors into the deep-submicron regime, MRS Bulletin. Vol.25. pp.18-21 (2000). <http://www.mrs.org/publications/bulletin>
- [2] Y. S. Lim, J. Y. Lee, H. S. Kim, D. W. Moon, Strain-induced diffusion in a strained $\text{Si}_{1-x}\text{Ge}_x/\text{Si}$ heterostructure, Appl. Phys. Lett. Vol.77. pp.4157-4159 (2000). <http://ojps.aip.org/aplo>
- [3] A. Portavoce, P. Gas, I. Berbezier, A. Ronda, J. S. Christensen, B. Svensson, Lattice diffusion and surface segregation of B during growth of SiGe heterostructures by molecular beam epitaxy: Effect of Ge concentration and biaxial stress, J. Appl. Phys. Vol.96, No.6. p.3158-3163 (2004).
- [4] I. Berbezier, A. Ronda, SiGe nanostructures, Surface Science Reports. Vol.64, pp.47-98 (2009). <http://dx.doi.org/10.1016/j.surfrep.2008.09.003>
- [5] E. Kasper, N. Burle, S. Escoubas, J. Werner, M. Oehme, K. Lyutovich, Strain relaxation of metastable SiGe/Si: Investigation with two complementary X-ray techniques, J. Appl. Phys. Vol.111, Art.No.063507. <http://dx.doi.org/10.1063/1.3694037> (2012).
- [6] T. A. Langdo, M. T. Currie, Z.-Y. Cheng, J. G. Fiorenza, M. Erdtmann, G. Braithwaite, C. W. Leitz, C. J. Vineis, J. A. Carlin, A. Lochtefeld, M. T. Bulsara, I. Lauer, D. A. Antoniadis, M. Somerville, Strained Si on insulator technology: from materials to devices, Solid-State Electronics, Vol.48. pp.1357-1367 (2004). <http://www.elsevier.com/locate/sse>
- [7] J. J. Hamilton, K. J. Kirkby, N. E. B. Covern, E. J. H. Collart, M. Bersani, D. Giubertoni, S. Gennaro, A. Parisini, Boron deactivation in preamorphized silicon on insulator: Efficiency of the buried oxide as an interstitial sink, Appl. Phys. Lett. Vol.91, Art.No.092122 (2007).
- [8] J. Bhandari, M. Vinet, T. Poiroux B. Previtali, B. Vincent, L. Hutin, J. P. Barnes, S. Deleonibus, A. M. Ionescu, Study of n-and p-type dopants activation and dopants behavior with respect to annealing conditions in silicon germanium-on-insulator (SGOI), Mat. Sci. Eng. B. Vols.154-155. pp.114-117 (2008).
- [9] P. Pichler, In: *Computational Microelectronics, Intrinsic point defects, impurities, and their diffusion in solids*, edited by S. Selberherr (Springer, Wien, New-York, 2004).
- [10] Y. Lamrani, F. Cristiano, B. Colombeau, E. Scheid, P. Calvo, H. Schäfer, A. Claverie, Direct evidence of the recombination of silicon interstitial atoms at the silicon surface, Nucl. Instrum. Meth. Phys. Res. B. Vol.216. pp.281-285 (2004).
- [11] International Technology Roadmap for Semiconductors. 2011 Edition. Front End Processes. P. 36. (<http://www.itrs.net/Links/2011ITRS/Home2011.htm>)

- [12] O. I. Velichko, A set of equations of radiation-enhanced diffusion of ion-implanted impurities, in: I. I. Danilovich, A. G. Koval', V. A. Labunov et al. (Eds.), Proceedings of VII International Conference "Vzaimodeistvie Atomnyh Chastits s Tverdym Telom (Interaction of Atomic Particles with Solid)", Part 2, Minsk, Belarus, pp.180-181 (1984) (in Russian).
- [13] H. D. Robinson, M. D. Deal, G. Amaratunga, P. B. Griffin, D. A. Stevenson, and J. D. Plummer, Modeling uphill diffusion of Mg implants in GaAs using SUPREM-IV, J. Appl. Phys. Vol.71. pp.2615-2623 (1992).
- [14] O. I. Velichko, Macroscopic description of the diffusion of interstitial impurity atoms considering the influence of elastic stress on the drift of interstitial species. Phil. Mag. Vol.88, No.10. pp.1477-1491 (2008).
- [15] V. A. Uskov and V. V. Vas'kin, Effect of nonuniform vacancy distribution on diffusion of impurities in semiconductors, Inorganic Materials. Vol.8, No.10. pp.1617-1618 (1972).
- [16] Ya. Morikawa, K. Yamamoto, K. Nagami, Uphill diffusion mechanism in proton-irradiated silicon, Appl. Phys. Lett. Vol.36, No.12. pp.997-999 (1980).
- [17] W. Akutagawa, H. L. Dunlap, R. Hart, O. J. Marsh, Impurity-peak formation during proton-enhanced diffusion of phosphorus and boron in silicon, J. Appl. Phys. Vol.50, No.2. pp.777-782 (1979).
- [18] O. I. Velichko, Modeling of the radiation-enhanced diffusion in silicon under conditions of proton bombardment, in: A. I. Bajin, V. E. Borisenko, M. I. Guseva, A. P. Zaharov et al. (Eds.), Proceedings of VI International Conference "Vzaimodeistvie Atomnyh Chastits s Tverdym Telom (Interaction of Atomic Particles with Solid)", Part 2, Minsk, Belarus, pp.44-47 (1981) (in Russian).
- [19] R. Krause-Rehberg, F. Borner, F. Redmann, Impurity gettering by vacancy-type defects in high-energy ion-implanted silicon at $R_p/2$, Appl. Phys. Lett., Vol. 77, No.24. pp. 3932-3934 (2000).
- [20] A. Peeva, R. Kögler, W. Skorupa, J. S. Christensen, A. Yu. Kuznetsov, Spatial distribution of cavities in silicon formed by ion implantation generated excess vacancies, J. Appl. Phys., Vol.95, No.9. pp.4738-4741 (2004).
- [21] A. F. Burenkov, F. F. Komarov, M. A. Kumakhov, M. M. Temkin, Tables of Ion Implantation Spatial Distribution, (Gordon and Breach, New York-London-Paris, 1986) 462 pp.
- [22] O. I. Velichko, *Simulation of coupled diffusion of impurity atoms and intrinsic point defects in semiconductor crystals D.Sc. thesis* (Belarusian State University, Minsk, Belarus, 1997) [In Russian].
- [23] O. I. Velichko, V. A. Dobrushkin, A.N. Muchynskij, V. A. Tsurko, V. A. Zhuk, Simulation of coupled diffusion of impurity atoms and point defects under nonequilibrium conditions in local domain, J. Comput. Phys. Vol.178(1). pp.196-209 (2002).

- [24] A. F. Burenkov, F. F. Komarov, M. A. Kumahov, and M. M. Temkin: Prostranstvennoe raspredelenie energii, vydelennoi v kaskade atomnyh stolknovenij v tverdyh telah (Space distribution of energy deposited in atomic collisions in solids), Energoatomizdat, Moscow (1985) [In Russian].
- [25] H. Strack, Ion bombardment of silicon in a glow discharge, J. Appl. Phys. Vol.34, No.8. pp.2405-2408 (1963).
- [26] O. I. Velichko, Microscopic mechanism responsible for radiation-enhanced diffusion of impurity atoms (to be published).
- [27] O. I. Velichko, A. P. Kavaliova, Modeling of the transient interstitial diffusion of implanted atoms during low-temperature annealing of silicon substrates, Physica B. Vol.407. pp.2176-2184 (2012).
- [28] Y. M. Haddara, B. T. Folmer, M. E. Law, T. Buyuklimanli, Accurate measurements of the intrinsic diffusivities of boron and phosphorus in silicon, Appl. Phys. Lett, Vol.77, No.13. pp. 1976-1978 (2000).
- [29] J. Chevallier, B. Pajot, Interaction of hydrogen with impurities and defects in semiconductors, Solid State Phenomena. Vol.85-86. pp.203-284 (2002).